AD A097625

HDL

Report

January 1981

Performance of the Fluidic Power Supply for the XM445 Fuze in Supersonic Wind Tunnels

by Richard L. Goodyear
Henry Lee

U.S. Army Electronics Research
and Development Command
Harry Diamond Laboratories
Adelphi, MD 20783

81 4 10

The findings in this report are not to be construed as an official Department of the Army position unless so designated by other authorized documents.

Citation of manufacturers' or trade names does not constitute an official indorsement or approval of the use thereof.

Destroy this report when it is no longer needed. Do not return it to the originator.

UNCLASSIFIED

SECURITY CLASSIFICATION OF THIS PAGE (When Data Entered)

REPORT DOCUMENTATION PAGE	READ INSTRUCTIONS BEFORE COMPLETING FORM
1 REPORT NUMBER: HDL TM 81-4	2 GOVT ACCESSION NO: AD-A097625
	3 RECIPIENT'S CATALOG NUMBER
4 TITLE (and Subtitle): Performance of the Fluidic Power Supply for the XM445 Fuze in Supersonic Wind Tunnels	5 TYPE OF REPORT & PERIOD COVERED: Technical Memorandum
	6 PERFORMING ORG REPORT NUMBER
7 AUTHOR(s): Richard L. Goodyear, Henry Lee	8 CONTRACT OR GRANT NUMBER(s)
9 PERFORMING ORGANIZATION NAME AND ADDRESS: Harry Diamond Laboratories, 2800 Powder Mill Road, Adelphi, MD 20783	10 PROGRAM ELEMENT PROJECT TASK AREA & WORK UNIT NUMBERS: Program Ele 6 33 03 A
11 CONTROLLING OFFICE NAME AND ADDRESS: Project Manager, Multiple Launch Rocket System, Redstone Arsenal, AL 35809	12 REPORT DATE: Feb 81
	13 NUMBER OF PAGES: 25
14 MONITORING AGENCY NAME & ADDRESS (If different from Controlling Office): (9) Technical memo,	15 SECURITY CLASS (of this report): UNCLASSIFIED
	15a DECLASSIFICATION DOWNGRADING SCHEDULE

16 DISTRIBUTION STATEMENT (of this Report)

Approved for public release, distribution unlimited

17 DISTRIBUTION STATEMENT (of the abstract entered in Block 20, If different from Report)

18 SUPPLEMENTARY NOTES

DRCMS Code 6433035640012
DA Project 1X463303D564
HDL Project 424006

19 KEY WORDS (Continue on reverse side if necessary and identify by block number)

Fluidic generator	Wind energy for fuze
Air driven generator	Rocket trajectory simulation
Power supply	Pressure measurements at rocket nose
Rocket fuze	Temperature measurements at rocket nose
MLRS	

20 ABSTRACT (Continue on reverse side if necessary and identify by block number)

As part of the development of the fluidic power supply of the XM445 fuze, wind tunnel tests of different configurations of the power supply were conducted at the Naval Surface Weapons Center in November 1979. Power supply performance and pressure and temperature measurements within the fuze were recorded at Mach 1.5 and Mach 5 for a range of pressures. Success or failure of any given configuration was based on degree of sensitivity at low pressure and ability to operate at high pressure and temperature. Measurements of temperature and pressure provided new information on conditions in the fuze.

DD FORM 1 JAN 73 1473 EDITION OF 1 NOV 65 IS OBSOLETE

UNCLASSIFIED

SECURITY CLASSIFICATION OF THIS PAGE (When Data Entered)

163030

CONTENTS

CONTENTS (Cont'd)

FIGURES

FIGURES (Cont'd)

TABLES

1. INTRODUCTION

Wind tunnel tests were conducted at the Naval Surface Weapons Center (NSWC), White Oak, MD, in November 1979. The purpose of these tests was to determine the performance of different fluidic generator configurations and to measure temperature and pressure at designated points within the XM445 fuze. These tests and the basic concepts and procedures were similar to those conducted in September 1978.[1]

2. TEST CONDITIONS

To simulate conditions at high altitude, tunnel 2 was used with a fixed Mach number of 1.5. Altitudes ranging from 9 to 21 km were obtained by varying total free stream pressure, P_{t1}, from 110 to 16.5 kPa. The squares in figure 1 show this test region compared with that of the Multiple Launch Rocket System (MLRS) M42 trajectory. To simulate conditions at rocket motor burnout, tunnel 8 was used with a fixed Mach number of 5. Consequently, only the stagnation temperature, T_0, and the total pressure, P_{t2}, behind the shock wave corresponding to point 1 in figure 1 could be duplicated. Although T_0 remained relatively constant, decreasing the free stream pressure permitted the matching of P_{t2} between points 1 and 2 in figure 1. Since the specified temperature is normally seen for only a few seconds in flight, it was necessary to insert the model into the stream at the temperature and the pressure of point 1 for 5 s, remove it for 5 s, and reinsert it for 5 s while the pressure was decreased to point 2. Actual durations were longer than 5 s due to the time required to raise and lower the model.

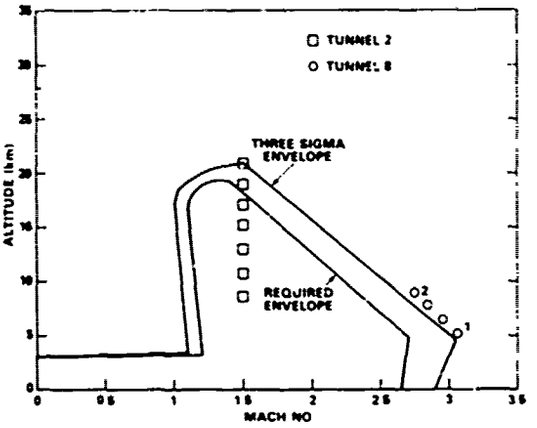

Figure 1. Multiple Launch Rocket System trajectories versus wind tunnel conditions.

3. ITEMS TESTED AND HARDWARE

The items tested and their hardware are listed here:

Standard Harry Diamond Laboratories (HDL) generator 790, to act as reference

Standard HDL generator 796, on which different nozzle configurations were tested

Generator with regulator produced by KDI Precision Products, Inc.

Brass nozzle 7 with KDI regulator (fig. 2)

HDL special generator S-2, with 0.457-mm (0.018-in.) reeds, 0.127-mm (0.005-in.) diaphragms, and 15-deg acoustic cavity offset by 90-deg step

HDL deflector 1, with adapter to standard nozzle (this deflector contained six holes (1.22 mm in diameter) drilled through it to enhance sensitivity.) (fig. 3)

[1] *Jonathan E. Fine, Performance of Ram Air Driven Power Supply for Proposed High Altitude Rocket in Naval Surface Weapons Center Supersonic Wind Tunnel, Harry Diamond Laboratories TM-80-31 (November 1980).*

HDL deflector. 2. with adapter to standard nozzle (fig. 4)

Standard electronics bundle 416. with 6 m of shielded cable for output signals (In addition to standard signal wires, unregulated dc voltage was brought out Access was provided to bridge rectifier by wire identified as Vb to facilitate calibration (fig. 5) This bundle and standard design differed.*) Thermocouples (T) installed (fig 6):

TA. on top of 2N6211 regulator transistor

TB. at center of terminal board

TC. at center of bottom of aluminum can

TD. on inside wall of can near terminal board

TE. on top of timer oscillator package

Standard ogive components except for dummy safety and arming (S&A) and detonator. thermocouples. and pressure taps (P) (fig. 6):

TF. in metal behind nose

TG. projecting into air near base of cone

TH. in metal near base of cone

P3. at small hole drilled between two existing exhaust holes such that measuring point is just at exit on cone's surface (Static pressure is measured.)

P4. at small hole drilled into center of cone's cavity such that measuring point is perpendicular to and on wall of inside of cone (Static pressure is measured.)

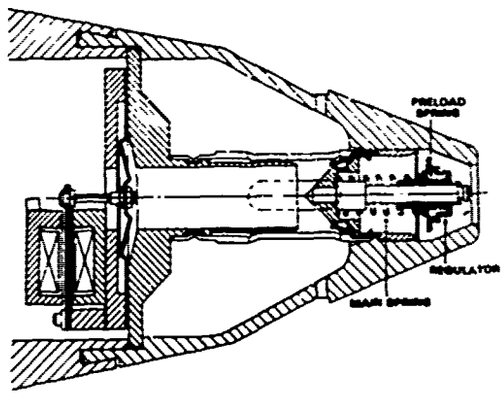

Figure 2. Concept of fluidic generator flow regulator.

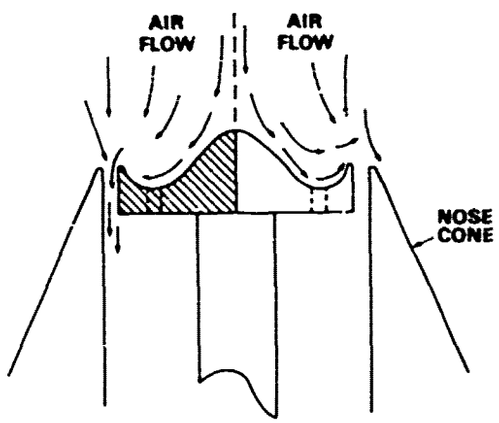

Figure 3. HDL flow deflector 1.

*Jerome Cooperman. *Modification of XM445 Fuze for NSWC Wind Tunnel Test.* Harry Diamond Laboratories (12 October 1979).

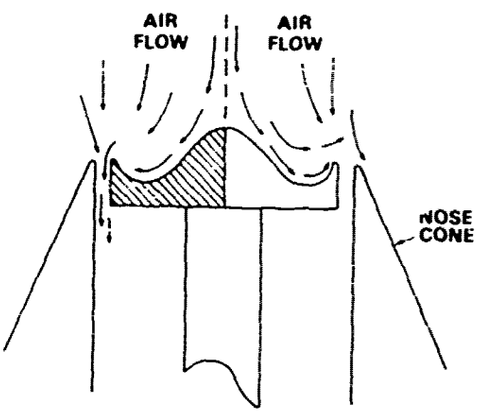

Figure 4. HDL flow deflector 2.

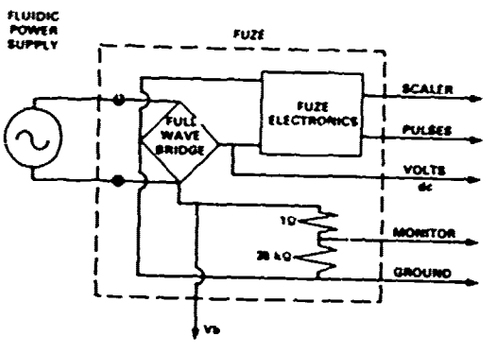

Figure 5. Fuze circuit with connections to power supply and instrumentation.

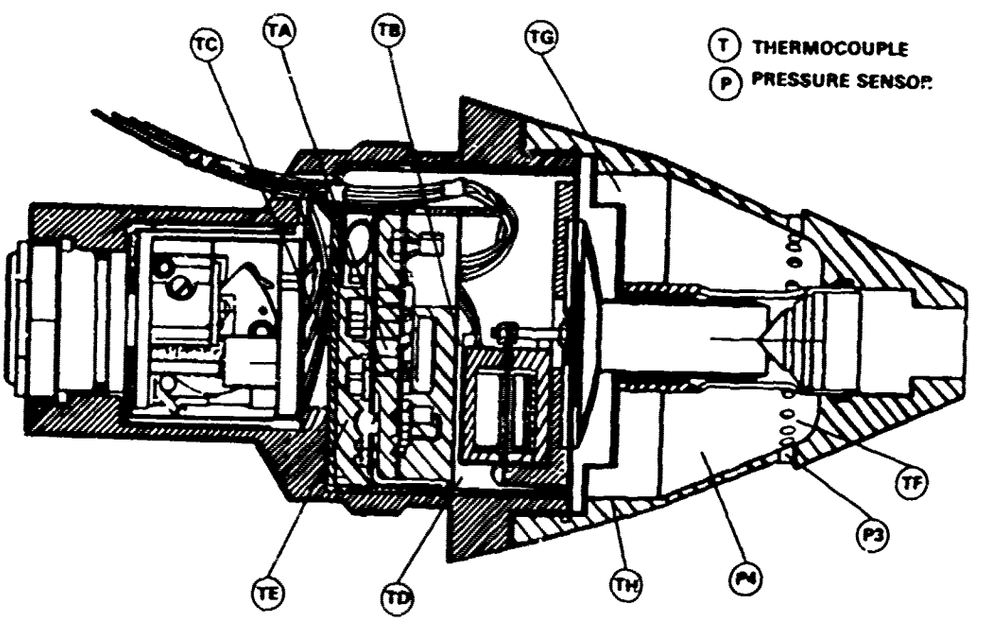

Figure 6. Locations of temperature and pressure transducers.

4. INSTRUMENTATION AND DATA ACQUISITION

Figure 7 shows the configuration of instruments and hardware applicable to both tunnels Additionally, the data acquisition system at NSWC recorded flow conditions in the tunnel, direct current (dc) voltage, pressure and temperature transducer signals, IRIG-B time code, and generator frequency. Schlieren photographs were taken of different fuze configurations Calibration of the system both in the laboratory and in the tunnels was similar; a signal generator introduced known signals of varying amplitudes into the fuze on the Vb wire while all instruments were operated. Therefore, the signals recorded by the measuring instruments could be correlated to actual performance of the fuze.

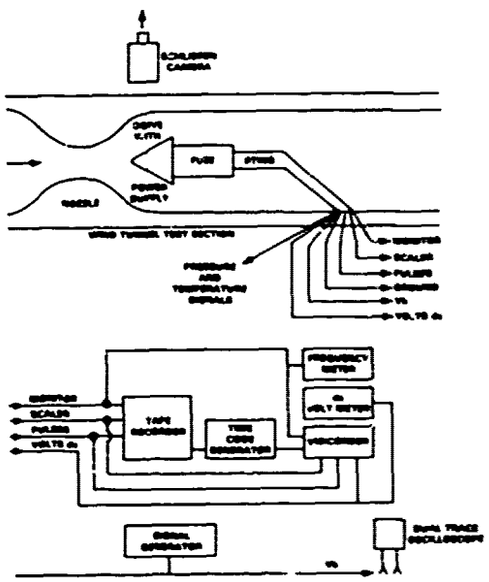

Figure 7. Apparatus for wind tunnel test.

5. GENERATOR PERFORMANCE IN MACH 1.5 SUPERSONIC WIND TUNNEL

5 1 *Test Configurations*

Five basic fluidic generator configurations were tested in the Mach 1.5 Supersonic Wind Tunnel to evaluate their voltage ouput characteristics as a function of dynamic pressure behind the shock wave, q_2. The configurations are these:

a. Standard generator
b. Standard generator with KDI flow regulator
c Standard generator with HDL flow deflector
d. Sensitive generator with KDI flow regulator
e. KDI production generator

The same fuze was used for all configuration tests Each of the generator configurations was evaluated in terms of its performance at low dynamic pressures, particularly the pressure required to generate the 23 Vdc needed to turn on the fuze. Each of the configurations was repeated in the wind tunnel testing to verify the consistency of the data obtained. The wind tunnel measured data were also compared with data obtained in the laboratory to provide a general correlation between the two measurement conditions.

5.2 *Test Results*

5.2.1 *Standard Generator*

Figure 8 is a plot of a standard generator voltage output measured in the wind tunnel versus that measured in the laboratory as a function of q_2, the dynamic pressure at the ogive inlet. The data show that fuze turn-on voltage of 23 Vdc was achieved in the wind tunnel at a q_2 of 7 45 kPa (1.05 psi)

as compared with a q_2 of 6.0 kPa (0.87 psi) in the laboratory. As q_2 increased, both traces appear to come to the same level. The NSWC wind tunnel fuze turn-on pressure measured for the standard generator compares closely with earlier test data at the National Aeronautics and Space Administration Ames Research Center, Moffett Field, CA, wind tunnel (fig. 9). The variation in voltage output noted at high pressures is due primarily to the reed adjustment tolerance between the generators.

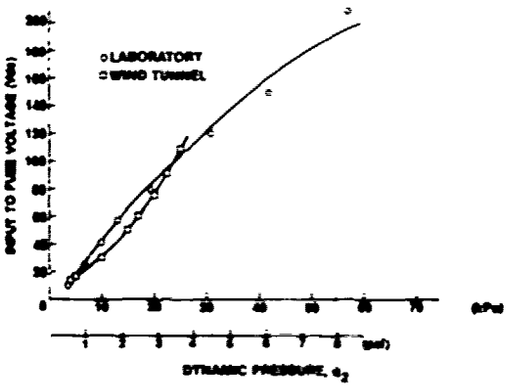

Figure 8. Standard generator 796 wind tunnel and laboratory measured voltages as function of dynamic pressure at ogive inlet.

5.2.2 *Standard Generator with Flow Regulators*

Figure 10 shows the effects of the regulator on the standard generator output performance. Both the KDI and HDL flow regulators were designed to reduce maximum voltage generated at high pressures without affecting the generator performance at low pressures. However, the wind tunnel data obtained show that the fuze turn-on pressure at which 23 Vdc was reached was increased from a q_2 of 7.25 kPa (1.05 psi) for a standard generator to 8.62 kPa (1.25 psi) when the HDL flow regulator was attached. This wind tunnel value matches closely with the fuze turn-on pressure measured in the laboratory, which was 8.30 kPa (1.20 psi). When the KDI flow regulator was attached to the standard generator, the fuze turn-on pressure measured in the wind tunnel was further increased to 10.76 kPa (1.56 psi). This represents an increase of almost 50 percent in q_2 needed to generate 23 Vdc. The tunnel data shown in figure 10 clearly indicate that the sensitivity of the standard generator was significantly reduced when flow regulators were used. The flow regulators were successful in reducing voltage output at higher pressures as desired. At a q_2 of 20 kPa, for example, the output was reduced from 80 Vdc for the standard generator to about 50 Vdc with the HDL regulator, and it was reduced further to 45 Vdc by the KDI regulator.

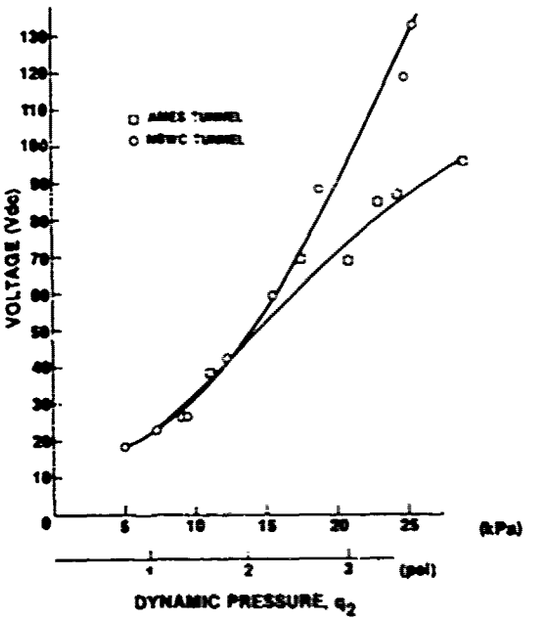

Figure 9. Ames Research Center and NSWC wind tunnel standard generator voltage outputs as function of dynamic pressure at ogive inlet.

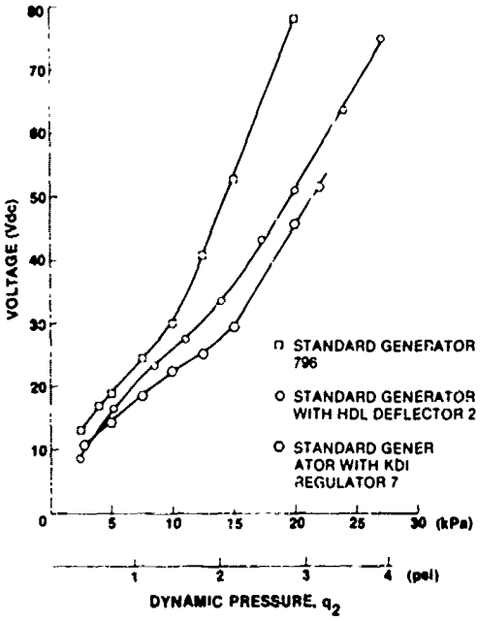

Figure 10. Fuze input voltage versus dynamic pressure at ogive inlet for three generator configurations.

Figure 11 compares the wind tunnel data with the laboratory data obtained from the standard generator with KDI flow regulator configuration. The fuze turn-on pressure measured in the tunnel is almost 50 percent higher than that measured in the laboratory. This wide variation between laboratory and wind tunnel data could be explained if aerodynamic conditions in the tunnel induced a lower pressure behind the regulator than existed in the laboratory for a given q_2 at the ogive inlet. The resulting higher pressure gradient across the regulator would cause the spring to compress further than in the laboratory. This extra spring displacement would create a corresponding reduction in flow area with less output voltage generated (sect 8.1 2).

Another configuration consisted of the standard generator with HDL flow deflector. The data obtained and shown in [illegible] 12 indicate that there is no appreciable [illegible]ence in voltage output data between this configuration and the configuration without the added inlet holes in the flow deflector. Figure 13 shows the wind tunnel data of voltage versus the q_2 of a standard generator with KDI regulator similar to the configuration described earlier, but with an extra large inlet in the ogive nose. The data obtained show no appreciable difference when compared with similar configurations in a standard ogive (fig. 11).

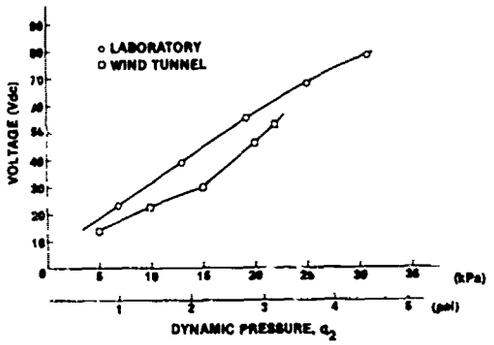

Figure 11. Laboratory and wind tunnel data of standard generator 796 with KDI regulator, voltage output versus dynamic pressure at ogive inlet.

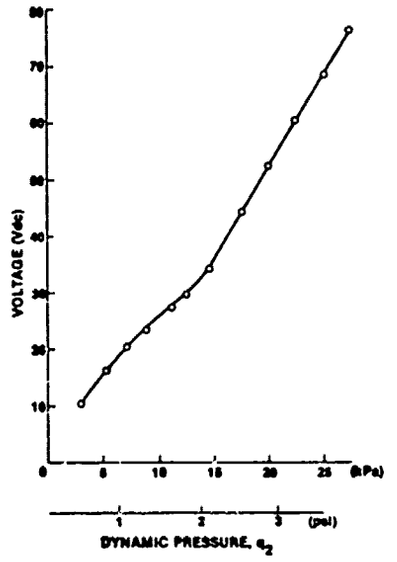

Figure 12. Standard generator with HDL flow deflector 1, voltage output versus dynamic pressure.

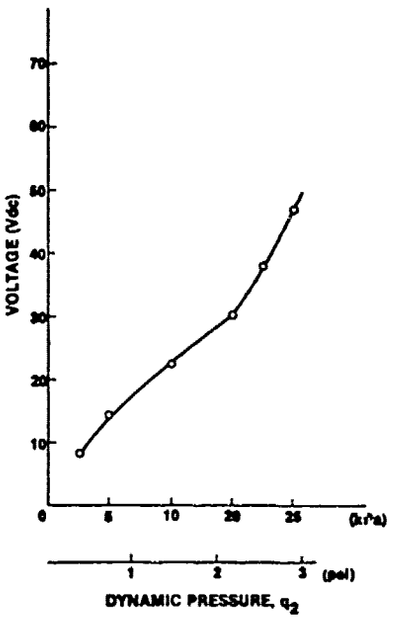

Figure 13. Standard generator 796 with KDI regulator inside large inlet ogive, voltage output versus dynamic pressure.

5.2 3 *S-2 Generator with KDI Flow Regulator*

Figure 14 is a plot of both the laboratory and wind tunnel data of a generator designed for improved sensitivity at low pressures, known as the S-2 generator. Only slight improvement was noted in the wind tunnel data. The fuze turn-on pressure of 9.73 kPa is about 10 percent less than the q_2 of 10.76 kPa measured for the standard generator with a KDI regulator.

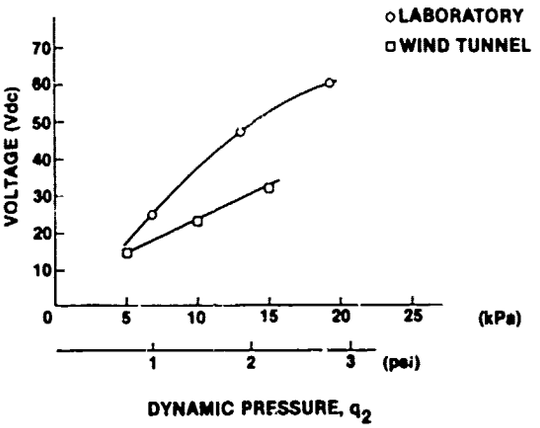

Figure 14. Laboratory and w nd tunnel data of S-2 generator with KDI regulator, voltage output versus dynamic pressure at ogive inlet.

5.2.4 *KDI Production Generator*

Figure 15 is a plot consisting of both the laboratory and wind tunnel measured voltage output as a function of q_2 for a KDI production model generator. The data show that a q_2 of 8.83 kPa (1.28 psi) was required to generate the fuze turn-on voltage of 23 Vdc in the wind tunnel. This indicates a 20-percent improvement in sensitivity when compared with the nonproduction generator with KDI flow regulator. Again, the wide variation noted between the laboratory and wind tunnel data at fuze turn-on pressures was due to aerodynamic effects that do not occur in the laboratory.

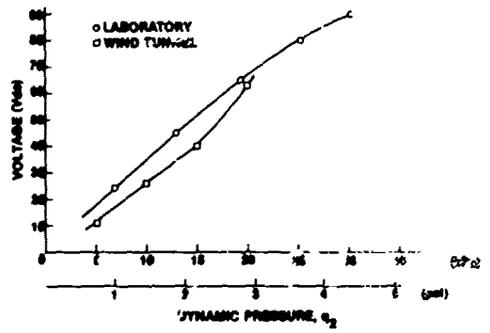

Figure 15. Laboratory and wind tunnel data of KDI production generator, voltage output versus dynamic pressure at ogive inlet (expanded scale).

5.3 *Summary*

The performance of the various generator configurations evaluated in terms of their sensitivity at low pressure is tabulated in table 1. The standard generator displayed the highest sensitivity. It turned on the MLRS fuze at a nominal q_2 of 7.25 kPa. This sensitivity was significantly reduced once flow regulators were used. The HDL flow deflectors appeared to be more sensitive than the KDI regulator, but they also appeared to act linearly, reducing voltage by the same percentage at low and high pressures. Although high pressure data are not available from the wind tunnel for the KDI regulator, it acts nonlinearly in the laboratory, reducing voltage significantly at high pressure (fig. 16). The standard generator with HDL flow deflector turned on the fuze at a q_2 of 8.62 as compared with a q_2 of 10.64 kPa required with the KDI regulator. Wind tunnel data on the sensitive generator (S-2) did not indicate that the design was an improvement over the standard generator as shown by the high value of q_2, 9.73 kPa, needed to turn on the fuze. The single KDI production generator appeared to have the same level of sensitivity as the standard generator with HDL flow deflector. Figure 17 shows the significance of these sensitivity data in terms of the MLRS trajectory envelopes over which the fuze must function. Although the standard generator does not fully meet the requirement, the addition of flow regulators seriously degrades performance.

Comparison of laboratory and wind tunnel data indicates that for the standard generator with HDL flow deflector, the measured values of fuze turn-on dynamic pressure q_2 are within 10 percent. For the same standard generator with KDI regulator, as well as KDI production generator, the wind tunnel data are almost 50 percent higher than laboratory data.

Also from table 1, a hysteresis effect in both the generator and the electronics causes the fuze to turn off at a lower pressure than at turn-on. The turn-on pressures calculated for recent Boeing Aerospace Co test flights of the MLRS are shown in table 2 and compare favorably with those in table 1.

6. GENERATOR PERFORMANCE IN MACH 5 SUPERSONIC WIND TUNNEL

6.1 *Test Configurations*

The same configurations tested in the Mach 1.5 tunnel were tested in the Mach 5 tunnel. The primary objectives were to evaluate the effects of the high stagnation temperature (approximately 450 C) and pressure (maximum P_{t2} of 620 kPa), as well as the ability of the regulators to perform as desired.

TABLE 1 SUMMARY OF GENERATOR PERFORMANCE IN TERMS OF FUZE TURN ON PRESSURE NSWC MACH 1.5 SUPERSONIC WIND TUNNEL

Configuration	Run No	Fuze turn on pressure q_2* (kPa)	(psi)	Fuze turnoff pressure q_2 (kPa)	(psi)
Standard generator [illegible]	1	[illegible]	1.0	–	
	4	[illegible]	[illegible]		
	*5	[illegible]	1.04	9.72	0.84
Standard generator 7x6	*6	7.4	1.08	6.67	0.98
Standard generator with HDL detector	*2	8.62	1.25	7.65	1.11
Standard generator with HDL detector with three holes	*1	8.41	1.22	7.58	1.07
Standard generator with KDI regulator	2	10.45	1.52	–	–
	9	10.76	1.56	8.79	1.27
	20	10.83	1.57	10.06	1.46
Standard generator with KDI regulator and large inlet ogive	*10	10.48	1.52	8.41	1.22
Sensitive generator (S2) with KDI regulator	*8	9.73	1.41	9.24	1.34
KDI production generator	7	8.62	1.25	6.89	1.00
	*9	8.55	1.24	7.86	1.14

*q_2 = dynamic pressure

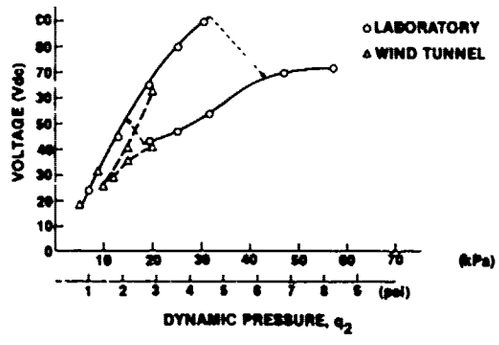

Figure 16. Laboratory and wind tunnel data of KDI production generator, voltage ouput versus dynamic pressure at ogive inlet.

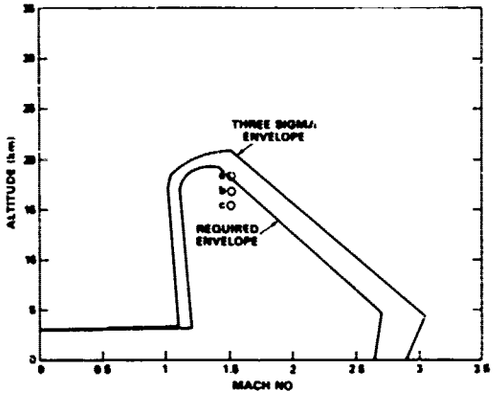

Figure 17. Multiple Launch Rocket System trajectories versus average turnoff altitude of fuze: (a) standard generator, q_2 = 5.89 kPa, 18.5 km; (b) KDI production generator, q_2 = 7.38 kPa, 17.1 km; standard generator with HDL regulator, q_2 7.52 kPa, 17 km; (c) standard generator with KDI regulator, q_2 = 9.41 kPa, 15.6 km (q_2 = dynamic pressure at ogive inlet).

TABLE 2. DYNAMIC PRESSURE, q_1, AT FUZE TURN-ON FOR RECENT BOEING FLIGHTS WITH TELEMETRY

Flight	Dynamic pressure at turn-on	
	(kPa)	(psi)
B-1	6 62	0 96
B-2	8 76	1 27
B-6	7 10	1 03
B-8	6 76	0 98
B-11	9 65	1 4
B-14	6 27	0 91
B-16	7 93	1 15
B-19	9 36	1 36
B-25	7 86	1 14
	Av 7 81	Av 1 13

6 2 *Test Results*

6.2 1 *Standard Generator*

Figure 18 shows the performance of generator 790, the dashed line reflects the gradual decrease in voltage as the frequency slowly rose, even though the pressure and the temperature remained relatively constant. Sufficient data to prepare a graph for generator 796 were not available since the sting on which the fuze was mounted failed to re-enter the tunnel as the pressure was reduced; however, the maximum voltage from the initial period in the tunnel was 267 V for the first 0 1 s, with a nominal value of 225 V.

6 2 2 *Standard Generator with Flow Regulators*

Figure 19 shows generator 796 with HDL flow deflector 1 with holes. The maximum voltage occurred for approximately 0 1 s upon initial insertion into the airstream, but the nominal value was approximately 255 V This reflects a 12-percent reduction in nominal peak voltage over the standard generator When HDL flow deflector 2 was used, the maximum voltage was 247 V for 0.1 s, and the nominal value was 200 V This nominal value reflects a 22-percent reduction in maximum voltage. When KDI brass regulator 7 was used, the springs failed under the temperature and pressure stresses, so initial voltage output was 36 V, with a drop below 23 V in 2 s

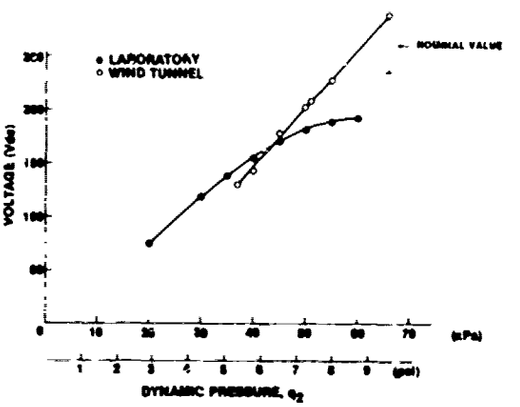

Figure 18. Laboratory and wind tunnel data of standard generator 790, voltage output versus dynamic pressure at ogive inlet.

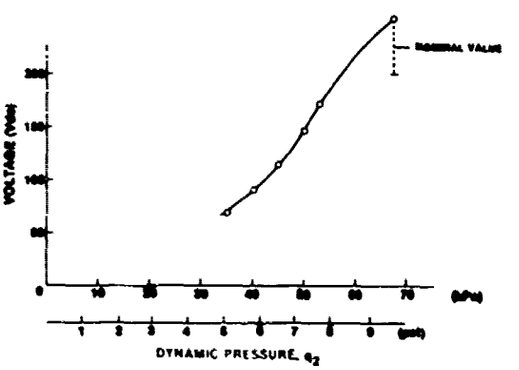

Figure 19. Laboratory and wind tunnel data of standard generator 796 with HDL flow deflector 1, voltage output versus dynamic pressure at ogive inlet.

6.2.3 *S-2 Generator with HDL Flow Deflector 2*

Figure 20 shows the performance of the S-2 generator with HDL flow deflector 2. No data for the generator without a regulator are available for comparison since this generator was designed to function with a KDI regulator. The nominal peak voltage was 125 V, a 50-percent reduction compared with the voltage of standard generators. Nevertheless, the output of this generator was noisier than others with obvious effects on the fuze timer.

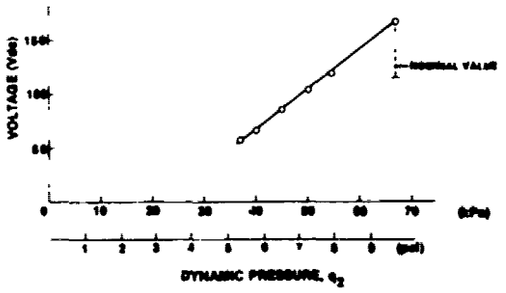

Figure 20. S-2 generator with HDL deflector 2, voltage output versus dynamic pressure at ogive inlet.

6.2.4 *KDI Production Generator*

Just as for brass nozzle regulator 7, the KDI production generator aluminum regulator failed. The initial voltage was 27 V, with a drop below 23 V in 0.3 s.

6.3 *Summary*

A comparison of the nominal, maximum voltages for each configuration in tunnel 8 is shown in table 3. Due to the failure of the springs in the KDI regulators, it was not possible to determine how these regulators would function during the early seconds of rocket flight. The other configurations performed as expected. The S-2 generator model appears to be unsatisfactory for high temperature and pressure operation because of the amount of noise in its output.

TABLE 3 PERFORMANCE OF TEST CONFIGURATIONS IN TUNNEL 8, MACH 5

Configuration	Max nominal voltage (Vdc)
Standard generator 790	260
Standard generator 796	255
Generator 796 with:	
HDL deflector 1 (2 holes)	225
HDL deflector 2	200
KDI regulator	Spring failed
KDI production generator	Spring failed
S-2 generator with HDL regulator 2	125*

*Adverse effects on scalar

7. RESULTS OF TEMPERATURE MEASUREMENTS

7.1 *Mach 1.5 Tunnel*

As can be seen in figure 21, the temperatures of the nose cone metal, TF and TH, follow the stagnation temperature, T_0; however, the temperature, TG, of the air in the cavity of the nose cone reflects the cooling effect of expanding the air through the system. This cooling effect is eventually overcome by the transfer of heat from the wall of the cone to the turbulent air inside; the latter part of the test run reflects this rapid increase in air temperature. Figure 22 shows that the heat transfer was probably aided by the decrease in mass flow rate as the driving pressure decreased. As expected, heating in and around the electronics can was minimal.

7.2 *Mach 5 Tunnel*

Figure 23 provides a prediction of the worst temperature conditions expected from the M42 MLRS, in which the extremely high temperatures exist for less than 10 s. Figure 24 shows the length of time that the model was actually in the airstream by indicating the frequency of the generator. During the first period in the airstream, the fre-

quency rises as the generator components are heated. During the second period, the frequency lowers as the driving pressure is lowered. Figure 25 shows the temperatures measured. As seen in figure 23, the sustained magnitude and duration of stagnation temperature, T_o, would not be experienced in flight so that a cooling effect would occur as T_o dropped below the temperature of the rocket nose. Again, there was insignificant change in the electronics package, while the metal of the nose cone followed T_o. But the large amount of turbulence and high wall temperature appear to have caused immediate and significant heating of the air in the nose cavity.

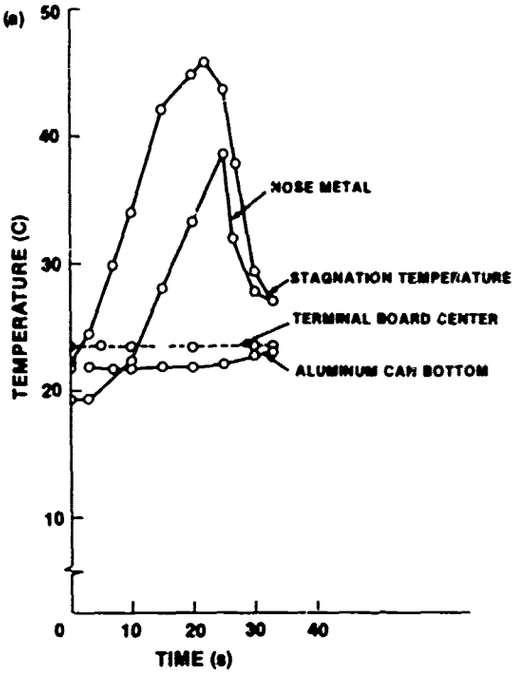

Figure 21. Temperatures recorded at Mach 1.5 for duration of run 15.

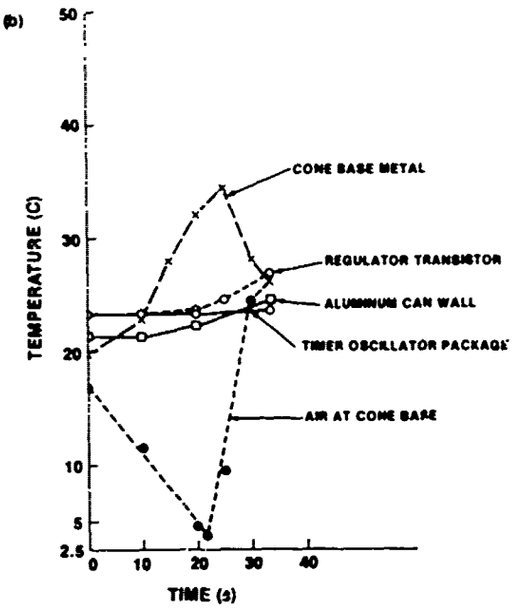

Figure 21. Temperatures recorded at Mach 1.5 for duration of run 15 (Cont'd).

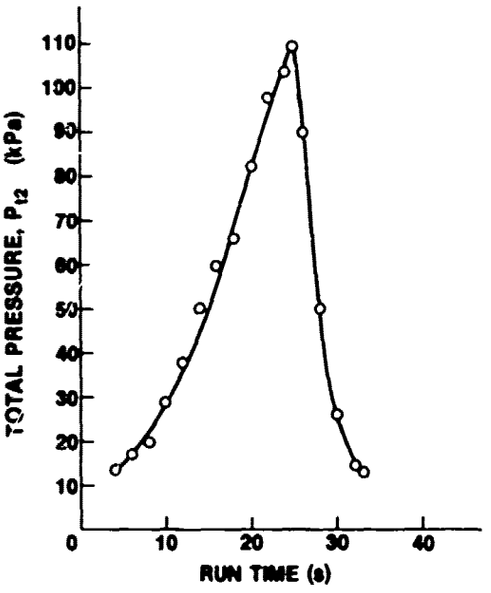

Figure 22. Total pressure at Mach 1.5 for duration of run 15.

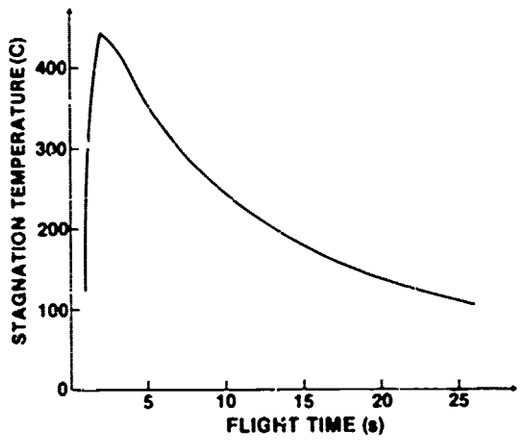

Figure 23. Multiple Launch Rocket System M42 trajectory prediction for worst temperature conditions: quadrant elevation = 10 deg, sea level launch, hot motor plus three standard deviations.

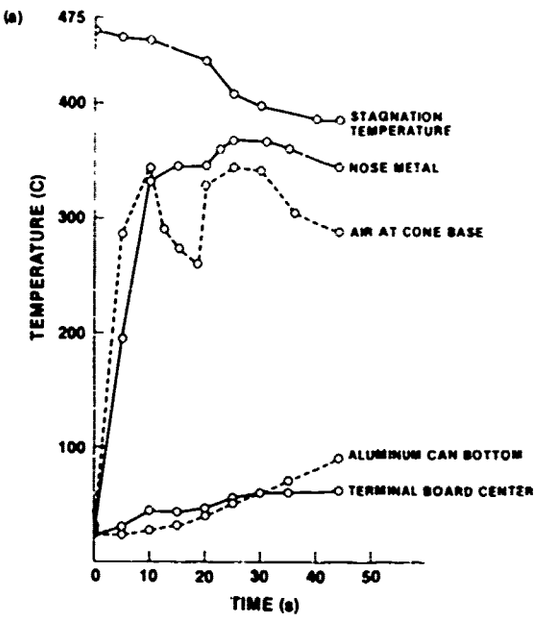

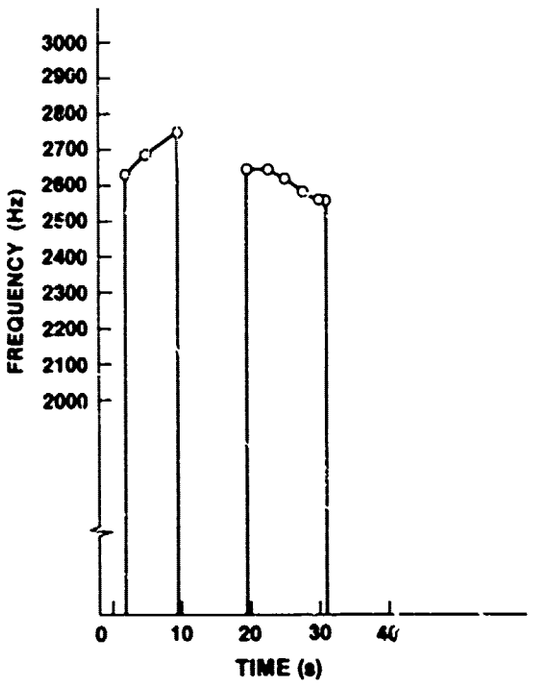

Figure 24. Generator output frequency for run 21.

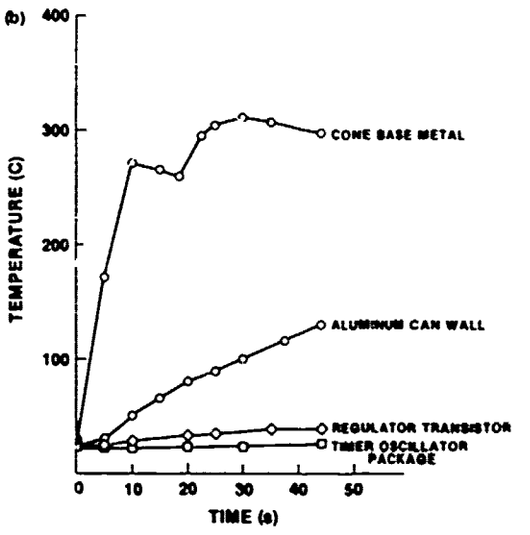

Figure 25. Temperatures recorded at Mach 5 for duration of run 21.

8. RESULTS OF PRESSURE MEASUREMENTS

8 1 *Mach 1 5 Tunnel*

8 1 1 *General Results*

Figure 26 shows static pressures P1 and P2 in front of and behind the shock wave, as well as the pressures at the exhaust holes, P3, and in the cavity, P4, all of which are referenced to P_{t2}, the total pressure behind the shock wave Although this figure reflects data from use of a standard generator, substitution of a KDI regulator made no difference Just as the relationship among P1, P2, and P_{t2} is constant at a given Mach number, it appears that the same is true for the cavity and exhaust pressures. The approximate ratios are $P4/P_{t2} = 0.55$ and $P3/P_{t2} = 0\ 47$ A significant result of the pressure measurements is that $q_2 = P2 - P3$

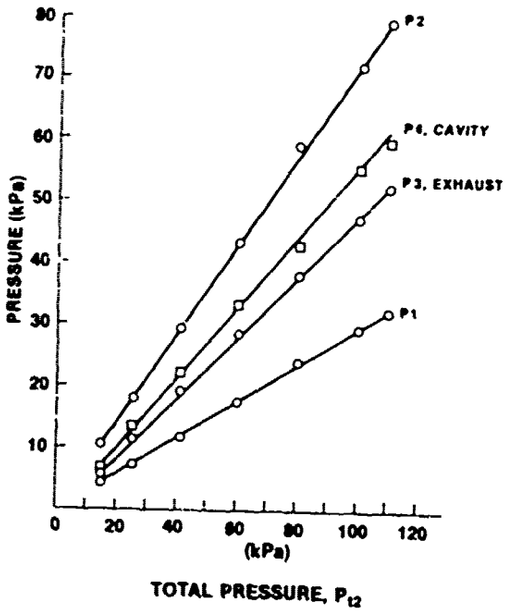

Figure 26. Pressure relationships at Mach 1.5.

8 1 2 *KDI Regulator Function*

In both the laboratory and the tunnel, instruments show that the small preload spring in the KDI regulator collapsed or snapped in at a certain pressure differential, allowing the regulator to suddenly reduce the flow rate into the nozzle Similarly, when the pressure differential was reduced to a certain value, the regulator snapped out again. Table 4 shows that in the laboratory the regulator snapped in and out at the given gauge pressure, which is the difference in total pressure at the entrance to the nozzle and the atmospheric pressure at the exhaust ports. These same pressure differences occurred in the wind tunnel for the same regulator function, except that the difference was obtained between the total pressure and the pressure inside the cone cavity. Figure 27 shows how KDI nozzle 7 performed at Mach 1.5; these same data are plotted against laboratory data in figure 28. One sees that the regulator functions occur at a lower dynamic pressure, q_2, in the wind tunnel. Dynamic pressure still appears to be a good key to predicting the voltage output when the regulator is collapsed. Figures 25 and 16 show the same relationships for the KDI production generator. Consider the phenomenon from a different perspective. In the wind tunnel at $q_2 = 6.27$ kPa, which corresponds to the fuze turn-on pressure in the laboratory, the pressure differential operating the regulator is $P_{t2} - P4 = 25.3 - 14.4 = 10.9$ kPa. However, in the laboratory at turn-on, the pressure differential operating the spring is the same as the dynamic pressure operating the generator. Therefore, in flight, the sensitivity of the KDI regulated generator must be less than that for a standard generator.

3 2 *Mach 5 Tunnel*

Figures 30 and 31 show the same pressure comparisons as presented for Mach 1 5 Figure 31 provides increased resolution on the P3 data of figure 29 Again, the rela-

tionship between pressures seems to be constant for a given Mach number. In this case, $P4/P_{t2} = 0.37$ and $P3/P_{t2} = 0.12$, but at these high pressures $q_2 << P2 - P3$. Hence, using q_2 to predict voltage output may suffice at low pressures, but not at high pressures.

9. SUMMARY OF WIND TUNNEL TEST RESULTS

The test was successful in that the relative sensitivity in terms of voltage as a function of pressure for various generator configurations was established. The standard HDL generator was most sensitive, while the addition of regulators decreased that sensitivity. The pressure corresponding to fuze initiation was slightly higher than that at turnoff, indicating a possible hysteresis effect.

The performance of the S-2 generator provided useful data for future design improvements. For the KDI regulators, the failure of the springs and the inconsistent behavior of the regulator itself gave the first evidence of inadequate design. The HDL regulators performed as expected Temperature measurements confirmed that the fuze electronics is unlikely to be affected by the high stagnation temperatures at the rocket's nose, but that heat must be considered in designing the generator or fuze ogive. Pressure data showed that the ratio between pressures in the fuze is fixed for a given Mach number. Hence, it may be possible to predict pressure from known free stream conditions; however, additional measurements at different Mach numbers would be necesssary to determine the proper mathematical functions for predicting pressures in the fuze.

TABLE 4. COMPARISON OF KDI REGULATOR FUNCTIONS AT MACH 1.5 WITH LABORATORY PERFORMANCE

Configuration	Snap-in (kPa)			Snap-out (kPa)		
	Laboratory	Tunnel		Laboratory	Tunnel	
	$P_g = P_{t2} - P3$	$P_{t2} - P4$	$P_{t2} - P3$	$P_g = P_{t2} - P3$	$P_{t2} - P4$	$P_{t2} - P3$
KDI production model	34 5	33 8	40 7	19 3	20 0	23.4
Nozzle 7	38 6	—	—	24.1	—	—
Run 2	—	45 5	53 1	—	24 1	27.6
Run 10	—	38.6	45 5	—	24 8	29 6

Notes

P_g = gauge pressure
P_{t2} = total pressure
P3 = exhaust pressure tap
P4 = cavity pressure tap

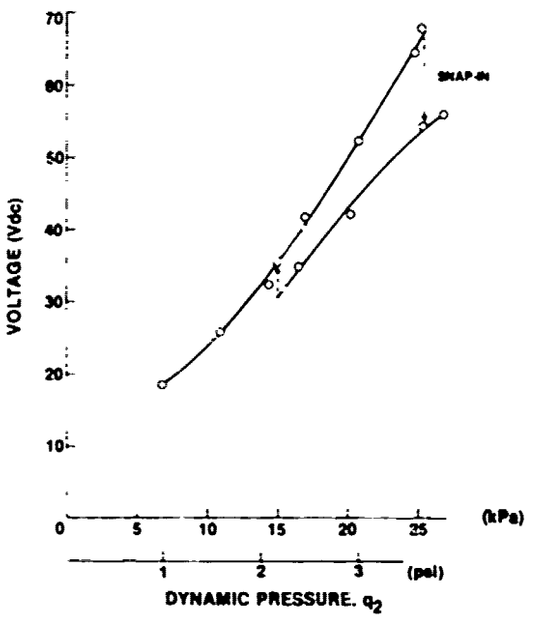

Figure 27. Wind tunnel performance at Mach 1.5 of generator 796 with KDI nozzle.

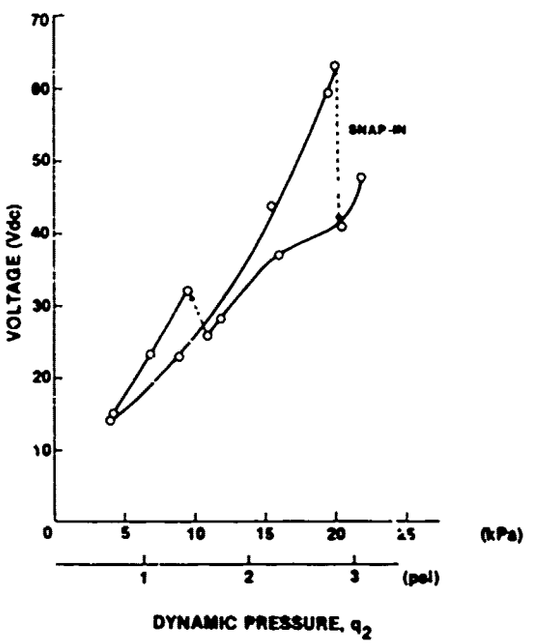

Figure 29 Wind tunnel performance of KDI production generator.

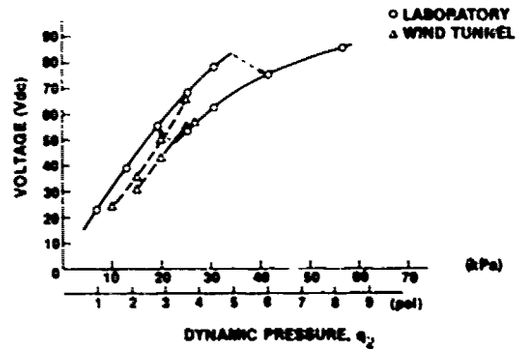

Figure 28. Laboratory and wind tunnel performance of generator 796 with KDI nozzle.

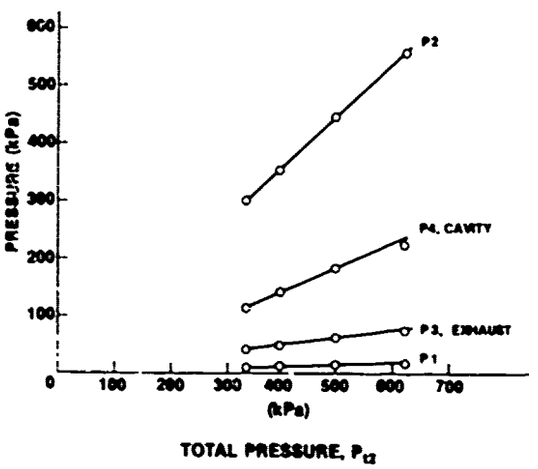

Figure 30. Pressure relationships at Mach 5 (1 psi = 6.8947 kPa).

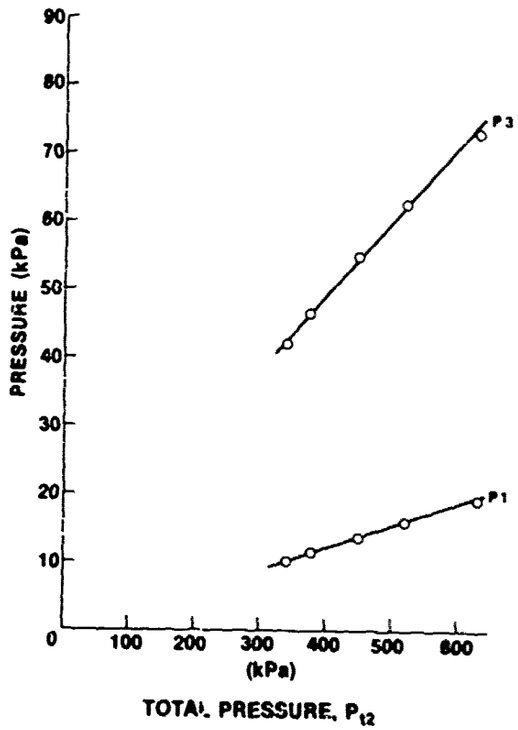

Figure 31. Pressure relationships at Mach 5, enlarged scale (1 psi ≈ 6.8947 kPa).

ACKNOWLEDGEMENTS

The authors acknowledge the assistance and the contributions of the following HDL personnel: Michael Salyards, who provided test models and instrumentation and assisted in data acquisition, Leroy Hughes, Jerome Cooperman, and Jonathan Fine, who assisted in troubleshooting problems, Don Robinson and the Field Test Branch, who provided backup magnetic tape records, Joe Knott and the NSWC wind tunnel staff, who provided outstanding cooperation in conducting the tests, and Carl Campagnuolo, for his guidance through all phases of the tests.

DISTRIBUTION

ADMINISTRATOR
DEFENSE TECHNICAL INFORMATION CENTER
ATTN DTIC-DDA (12 COPIES)
CAMERON STATION, BUILDING 5
ALEXANDRIA, VA 22314

COMMANDER
US ARMY RSCH & STD GP (EUR)
ATTN CHIEF, PHYSICS & MATH BRANCH
FPO NEW YORK 09510

COMMANDER
US ARMY ARMAMENT MATERIEL
READINESS COMMAND
ATTN DRSAR-LEP-L, TECHNICAL LIBRARY
ATTN DRSAR-ASF, FUZE AND MUNITIONS
SUPPORT DIV
ROCK ISLAND, IL 61299

COMMANDER
US ARMY MISSILE & MUNITIONS
CENTER & SCHOOL
ATTN ATSK-CTD-F
REDSTONE ARSENAL, AL 35809

DIRECTOR
US ARMY MATERIEL SYSTEMS ANALYSIS
ACTIVITY
ATTN DRXSY-MP
ABERDEEN PROVING GROUND, MD 21005

DIRECTOR
US ARMY BALLISTIC RESEARCH LABORATORY
ATTN [illegible]
ABERDEEN PROVING GROUND, MD 21005

US ARMY ELECTRONICS TECHNOLOGY
AND DEVICES LABORATORY
ATTN DELET-DD
FORT MONMOUTH, NJ 07703

HQ USAF/SAMI
WASHINGTON, DC 20330

[illegible] BROWN ENGINEERING
[illegible]MMINGS RESEARCH PARK
ATTN DR. MELVIN L. PRICE, MS-44
HUNTSVILLE, AL 35807

COMMANDER
US ARMY MISSILE COMMAND
ATTN DRCPM-RS, MLRS (B. CROSSWHITE)
REDSTONE ARSENAL, AL 35809

COMMANDANT
US ARMY WAR COLLEGE
ATTN LIBRARY
CARLISLE BARRACKS, PA 17013

SUPERINTENDENT
[illegible], USMA
ATTN TECHNICAL LIBRARY
WEST POINT, NY 10996

COMMANDER
NAVAL SURFACE WEAPONS CENTER
ATTN R. VOISINET
ATTN E-40, TECHNICAL LIB
WHITE OAK, MD 20910

US ARMY ELECTRONICS RESEARCH
& DEVELOPMENT COMMAND
ATTN TECHNICAL DIRECTOR, DRDEL-CT

HARRY DIAMOND LABORATORIES
ATTN CO/TD/TSO/DIVISION DIRECTORS
ATTN RECORD COPY, 81200
ATTN HDL LIBRARY, 81100 (3 COPIES)
ATTN HDL LIBRARY, 81100 (WOODBRIDGE)
ATTN TECHNICAL REPORTS BRANCH, 81300
ATTN CHAIRMAN, EDITORIAL COMMITTEE
ATTN LEGAL OFFICE, 97000
ATTN CHIEF, 34400
ATTN CHIEF, 34600
ATTN CHIEF, 34000
ATTN CHIEF, 13400
ATTN DEADWYLER, S., 13400
ATTN FINE, J., 34600
ATTN FINGER, D., 34400
ATTN MORROW, D., 34400
ATTN COOPERMAN, J., 34400
ATTN GOTTRON, R., 13400
ATTN GOODMAN, R., 34400
ATTN WESTLUND, R., 47000
ATTN GOODYEAR, R., 34600 (10 COPIES)
ATTN LEE, H., 34600 (5 COPIES)